Bridging of an Isolated Polymer Chain

Jorge Jimenez,[†] Jason de Joannis,[†] Ioannis Bitsanis,[‡] and Raj Rajagopalan*[,†]

Department of Chemical Engineering, University of Florida, Gainesville, Florida 32611-6005, and Foundation for Research and Technology−Hellas, Institute of Electronic Structure & Laser, P.O. Box 1527, Heraklion 711 10, Crete, Greece

Received March 29, 2000; Revised Manuscript Received June 26, 2000

ABSTRACT: Lattice Monte Carlo simulations are used to analyze a single polymer chain in good solvent confined between two adsorbing walls. Results are reported for the number and size distribution of bridge conformations and the resultant attractive force between the surfaces as a function of intersurface distance, H, and the effective adsorption energy, ϵ, between the polymer segment and the wall. The results are consistent with indirect experimental measurements of bridging in a multichain system and additionally yield information on the mechanism of bridging. In the case of single chains and strong adsorption ($\epsilon > 0.5\ k_BT$), the force per bridge f_{br} is independent of separation and depends only on the adsorption energy, in agreement with scaling analysis. In the case of weak adsorption (or for multichain systems) it is explicitly shown that steric interactions (loop−loop, loop−bridge interactions, etc.) are important. The "force per bridge" again has a roughly constant magnitude (appropriately diminished by steric interactions) but cannot be related unequivocally to the adsorption energy at the surface.

1. Introduction

The structure of polymer layers and the forces arising from the interaction of a polymer layer with another surface are of importance in a number of scientific and technological applications. In a recent communication we considered a single homopolymer chain confined between two athermal walls and examined the conformation of the chain and the force due to confinement.[1] This was motivated by the fact that the correct fundamental description of single chains at interfaces enhances one's understanding of more realistic many-chain problems of direct technological relevance. Also important in this context are interactions with adsorbing walls or with undersaturated layers. In both cases, the so-called bridging interactions play a notable role. A bridge is a section of a polymer chain that is attached (either physically adsorbed or chemically grafted) to two different bodies often idealized as flat parallel plates. Understanding the mechanism for bridging is crucial for controlling the quality of adhesives. Bridge formation is also important in colloid stabilization, or rather destabilization by flocculation, and crystallization of molten polymer (i.e., final morphology depends on bridging between crystalline seeds).

Models of bridging in a variety of multichain systems have used mean-field,[2−10] scaling,[2,4−6,11,12] and Monte Carlo[13−15] methods. Evidence for the attractive forces caused by bridging has been obtained by measuring directly the forces between two surfaces using the surface force apparatus (SFA)[16,17] and atomic force microscopy (AFM)[18] and indirectly from neutron diffraction experiments on suspensions.[19,20] In the measurements reported recently by Swenson et al.,[19,20] the effect of adding poly(ethylene oxide) (PEO) to an aqueous/clay suspension is analyzed. The magnitude of the polymer-related forces is inferred from accurately measured decreases in colloidal spacing after addition of PEO. The flat geometry of the clay particles makes it an ideal system for a bridging analysis. On the basis of an estimate of the number of bridges formed per unit area, the authors suggest that a *constant* force per bridge of roughly 1.4 pN develops in the system under equilibrium conditions.

There are fewer theoretical[5,21,22] and experimental[23−25] studies on the simpler case of the bridging interactions of an *isolated* chain. Single-chain bridging may be considered insignificant under conditions typically realized in technological applications. However, even in such cases single-chain events could play a role in the early stages of a process. For instance, measurements of the total adsorbed amount[26] of polymers from dilute solutions are high enough to indicate that the surface is still characterized by a high degree of chain interactions, although the polymer chains in the bulk solution do not overlap. Nevertheless, it is possible to have isolated chains at the surface for an appreciable amount of time before equilibrium is reached in many systems.[27] Biological systems also exhibit more frequently bridging interactions due to single biopolymer chains.

DiMarzio and Rubin[21] were the first to study bridge formation, using an isolated ideal chain. Their matrix formalism, which was extended and used to treat multichain systems by Scheutjens and Fleer,[10] provided early numerical results for the distribution of bridges and force as a function of separation and adsorption energy. More relevant is the scaling analysis of Ji et al.,[5] in which analytical results, valid for good solvent conditions, are obtained for the average size and number of bridges. A combination of these results with the assumption that each bridge is individually governed by the Pincus law of elasticity[28] yields a force per bridge that is independent of separation between the surfaces—much like the neutron diffraction results mentioned above. The scaling analysis of Ji et al. also predicts that the force per bridge, f_{br}, scales with adsorption energy as

$$f_{br} \sim \left(\frac{\epsilon_0}{a}\right)^{3/2} \quad (1)$$

[†] University of Florida.
[‡] Institute of Electronic Structure.

10.1021/ma000564n CCC: $19.00
Published on Web 08/23/2000

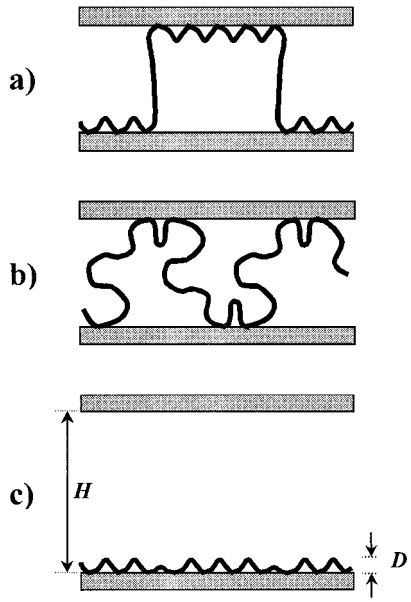

Figure 1. Single chain confined between two adsorbing walls: (a) large ϵ, (b) small ϵ, (c) limit of large ϵ and H. The average loop extension D is shown schematically in (c).

where ϵ_0 is the effective theoretical adsorption energy and a is the size of a segment or a repeating unit.

Several illustrations (meant as caricatures) of a single adsorbed chain are shown in Figure 1a−c. The first case (Figure 1a) corresponds to a system with strongly adsorbing surfaces such that there are relatively few bridges, and these are, in general, highly stretched. Most of the chain is tightly adsorbed to the surface in short loop conformations. This is usually referred to as the strong-stretching bridge regime, and it will constitute the primary consideration of this paper. Strong stretching is easier to model since the role of loop conformations may safely be ignored, and only the elasticity of noninteracting bridges needs to be accounted for, as was suggested by Ji et al.[5]

A weak-stretching regime (Figure 1b) occurs when the surfaces are less adsorptive. This is characterized by a large number of slightly stretched bridges and fewer, but larger, loop conformations. Finally in the limit of large separation and adsorption energy, the chain adsorbs only onto one wall (Figure 1c). Tail conformations (unadsorbed ends of the chain) become irrelevant when the chain length is sufficiently large.[29]

A full understanding of the bridging force and interactions requires additional details such as number of bridges and possible interaction of the bridges with loops and tails of the chain. To our knowledge there have been no computer simulations that attempt to study directly the force induced by a *single* polymer chain that adsorbs onto two parallel surfaces. Here, we present a lattice Monte Carlo study of this problem using a recently developed computational technique to determine the force induced by bridges. One of our objectives is to test the predictions of the scaling analysis presented by Ji et al.[5] In addition, we examine in detail whether there is any effect due to interactions between bridges of a single chain, the distribution of bridge sizes, and possible interference from loop conformations. We also provide a scaling analysis for the retraction of a strongly adsorbing single chain in a good solvent. Finally, we also comment briefly on bridging interactions in multichain systems.

2. Simulation Method

Polymer chains are modeled as confined self-avoiding walks (SAW's) inscribed on a simple cubic lattice. Steps into either surface layer are favored by a Boltzmann factor $\exp(-\epsilon/k_BT)$. The number of steps, N, in each SAW is chosen as 1000, corresponding to a very long polymer chain, for which scaling laws should hold. On the basis of our experience from neutral-wall simulations, this chain length proved to be sufficient to test the scaling limit.[1] If the direction, z, is normal to both surfaces, the discrete surface−segment potential is

$$\begin{aligned} U_{ext} &= \infty \qquad z < 1,\ z > H \\ &= -\epsilon \qquad z = 1,\ z = H \\ &= 0 \qquad 1 < z < H \end{aligned} \tag{2}$$

The method used for sampling of the SAW's is based on the "configurational bias" algorithm of Siepmann and Frenkel.[30] This method consists of breaking an existing chain configuration into two parts, erasing one of these subchains, and randomly regrowing it using an algorithm based on the well-known Rosenbluth−Rosenbluth method.[31] The force exerted by the polymer chain, f, is estimated from the change in Helmholtz potential, F, that occurs when the separation between the walls is decreased from H (state 1) to $H - 1$ (state 2), i.e.,

$$f(H - {}^1/_2) = \frac{\partial F}{\partial h}|_{H-1/2} \approx F(H-1) - F(H) \tag{3}$$

defined so that a negative force implies an attraction between the walls. Here, h is used to represent the wall separation as a free variable.

The Helmholtz potential difference in eq 3 is obtained using the recently developed contact-distribution method (CDM).[32] The starting point of this method is the acceptance-ratio technique introduced in the 1970s by Bennet,[33] which provides a Monte Carlo formalism for obtaining the difference in the Helmholtz potential between two systems that are physically identical but have different energy fields (e.g., different pair potentials or external potentials). The contact-distribution method takes advantage of Bennet's approach to treat the case of the interaction of a solid object with the polymer chains (in the present case, moving an object or a surface relative to the chains). The problem of moving a "hard" wall (or, in general, the boundary of a solid object) is equivalent to considering two systems with identical potential fields except in the layer immediately adjacent to the moving wall (say, the "surface layer"). At the surface layer an external potential, U_{ext}, ranging from 0 to ∞ is applied,[34] with the application of the infinite potential signifying the relocation (i.e., moving) of the wall to the location of the original surface layer. To obtain the Helmholtz energy difference, CDM requires the determination of the distribution of the number of contacts between the polymer chains and the moving object, that is, the probability, $p(m)$, of finding m segments in the surface layer. As the Helmholtz potential is a state function, the actual path taken is immaterial and can, in fact, be "unphysical". The path required in CDM when the moving wall is *adsorptive* is more circuitous than in the case of a "hard" wall and consists of three steps: (i) desorption of the chain from one of the walls (taken to be the upper one here), (ii) moving that wall to the new position, and (iii) readsorption of the chain back on that wall. To achieve this,

Table 1. Force Induced by a Single Polymer Chain at Different Adsorption Energies, ϵ

	ϵ/k_BT					
H/a	0.3	0.5	0.6	0.75	0.85	1.0
4.5	−4.65	−16.69	−21.24	−23.84	−23.65	−22.19
5.5	−0.55	−11.08	−12.21	−12.63	−10.84	−7.79
6.5	−0.21	−6.80	−7.58	−6.22	−4.86	−3.36
7.5	−0.37	−4.60	−5.30	−3.15	−2.54	−2.03
8.5	−0.66	−3.28	−2.48	−1.13		
9.5	−0.12	−2.82	−0.95			
10.5	−0.58					

the calculation requires the use of a sequence of fictitious potentials $U_{ext}(z=H)$ at the upper surface. During step i, $U_{ext}(H)$ is gradually increased (in increments of $\delta\epsilon > 0$) starting from $-\epsilon$ until the probability of zero surface contacts is obtained accurately. In particular, this proceeds as follows. One changes the external potential in steps, i.e., $U_{ext} = -\epsilon$, $U_{ext} = -\epsilon + \delta\epsilon$, $U_{ext} = -\epsilon + 2\delta\epsilon$, ..., and determines the distribution of segments in the surface layer (and, therefore, the probability of contacts) at each stage. The number of such increments needed depends on the conditions of the experiment (such as number of chains, separation distance between the plates, and the original magnitude of the adsorption energy); see, for details, ref 32. Once $p(0)$ is determined with sufficient accuracy, the corresponding change in Helmholtz potential is obtained as described in ref 32. The probability of zero surface contacts determined in this manner characterizes the free energy change when the adsorptive surface moves by one lattice unit and simultaneously becomes nonadsorptive. In step ii a new system of width $H - 1$ is generated. Step ii therefore corresponds to a chain in equilibrium with one adsorptive wall (the lower one) and one nonadsorptive wall (the upper one). Finally, in step iii the surface potential at the upper wall, $U_{ext}(H - 1)$, is gradually decreased[36] from 0 to $-\epsilon$, so that the chains are readsorbed at that wall. The net effect of these three steps is to go from two adsorptive walls at a distance of H to two adsorptive walls separated by a distance of $H - 1$. The sum of the free energy changes obtained in these three steps is, therefore, the desired total change in the Helmholtz energy.

A snapshot of the bridges in a typical case is shown in Figure 2a,b. The forces arising from bridging have two competing factors. Attractive forces arise from the tension in bridge structures, and repulsive forces arise from excluded-volume interactions and the entropic cost of confining the chains. In Table 1 the forces are listed for adsorption energies ranging from 0.3 to 1.0 k_BT for separations between the surfaces, H/a (with a being the size of the lattice unit), ranging from 4 up to the separation at which bridging ceases (between 7 and 11). Separations below approximately 4 lattice units exhibit a deviation from universal (i.e., lattice independent) behavior in some[37] but not all of the system properties.

3. Discussion

In what follows, we first focus on the number of bridges as a function of separation between the walls and the force due to the bridges. The latter will also be compared with results based on scaling arguments. Following this we shall examine the distribution of bridges in terms of size and under what conditions steric interactions between the bridges and the rest of the chain and the effects of exclusion of conformations by the wall set in. Finally, we present a scaling argument for the force of retraction of an adsorbed chain and compare it with the bridging forces observed in the simulation.

3.1. Number of Bridges. In Figure 3, the number of bridges, n_{br}, is plotted as a function of H/a for a sequence of adsorption energies. The trend seen is consistent with the numerical results of DiMarzio and Rubin,[21] which predict that the number of bridges vanishes when the adsorption energy becomes overwhelming and the chain adopts completely flattened conformations. At each separation, a maximum in the number of bridges must occur at a certain ϵ that is somewhere between strongly adsorptive and repulsive. Figure 3 suggests that this maximum occurs at a magnitude of ϵ below 0.5 k_BT for all of the separations shown since none of the curves overlap. The decrease of the number of bridges with separation, shown in Figure 3, is consistent with the exponential decay of the scaling prediction:[5]

$$n_{br} \sim N\left(\frac{D}{a}\right)^{-5/3} \exp(-H/2D) \tag{4}$$

where D is a length comparable to the average loop extension (Figure 1c) and depends only on the adsorption energy.

3.2. Bridging Forces. For all $\epsilon > 0.3\ k_BT$, the magnitude of the observed force (see Figure 4) decreases monotonically with increasing separation between surfaces. For the lowest energy, $\epsilon = 0.3\ k_BT$, the force fluctuates near zero for large separations and becomes slightly attractive for small separations. This indicates that the system is close to the "threshold" adsorption energy, defined as the point at which the volume fraction profile becomes uniform (the adsorption energy at which the energetic profit is exactly balanced by the entropic cost for the chain to assume an adsorbed conformation).[38] In what follows we examine adsorption energies in the range between 0.5 and 1.0 k_BT. As we have noted earlier, one might idealize the system as two planes connected by several elastic tethers individually governed by the Pincus law, which will be described later (see eq 6 and the following discussion). This model ignores possible repulsive contributions arising from loop conformations and the interaction between bridges that might alter their collective elasticity. With this in mind, it is interesting to study the force f_{br} per bridge, i.e., the ratio of the total force and the number of bridges obtained from the simulation:

$$f_{br}(H - {}^1/_2) = \frac{f(H - {}^1/_2)}{n_{br}(H - {}^1/_2)} \tag{5}$$

Note that this calculation requires interpolation of the number of bridges since n_{br} is obtained at integer valued separations: H and $H - 1$. The uncertainty introduced in the values of f_{br} by the interpolation of n_{br} is not expected to be of major concern since the n_{br} data are relatively smooth.

The force per bridge, f_{br}, is plotted as a function of H in Figure 5a and as a function of ϵ in Figure 5b. These results yield *direct* evidence that there is a constant force per bridge. The observed relation between the force per bridge and the adsorption energy is in very good agreement with eq 1. This result suggests that the interaction between different bridges does not play a major role and that the forces are simply additive. A

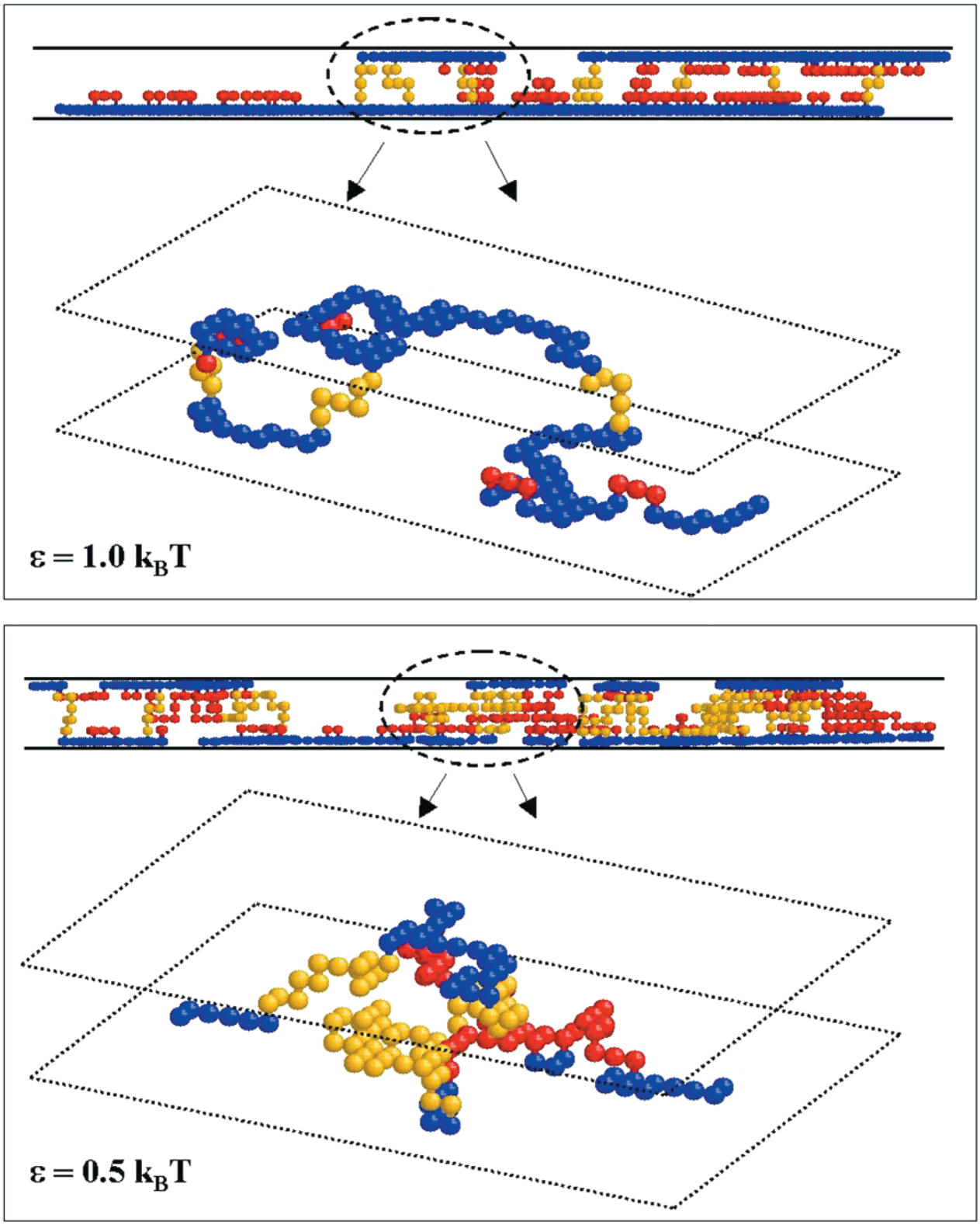

Figure 2. Snapshots from a simulation showing a side view (2-D projection) of a chain and a 3-D perspective of a section of the chain. The blue segments denote adsorbed segments or trains, the red segments are the loops, and the yellow ones belong to bridges. Case a (top) corresponds to $H = 5$ and $\epsilon = 1.0\ k_BT$, and case b (bottom) to $H = 6$ and $\epsilon = 0.5\ k_BT$.

more careful examination of this statement is presented below, where we analyze the distribution of the bridge sizes for a number of adsorption energies.

3.3. Distribution of Bridges. The interpretation of the results presented in the previous section is facilitated by the size distribution of the bridges obtained for various adsorption energies. Figure 6 shows the probability that a bridge has a certain degree of stretching, H/R_F. Here R_F is the root-mean-squared end-to-end length of an unperturbed chain with as many segments as are in each bridge (known as the natural length of the bridge). This length is characterized by the well-known Flory exponent, $R_F \sim N^{3/5}$, where the prefactor depends on the model.[39] In other words, what is plotted

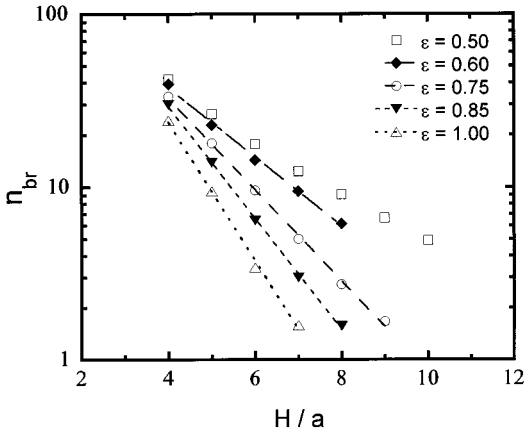

Figure 3. Number of bridges, n_{br}, as a function of the separation between surfaces, H/a (where a is the lattice spacing). Exponential trend lines are shown for $\epsilon > 0.5\ k_BT$.

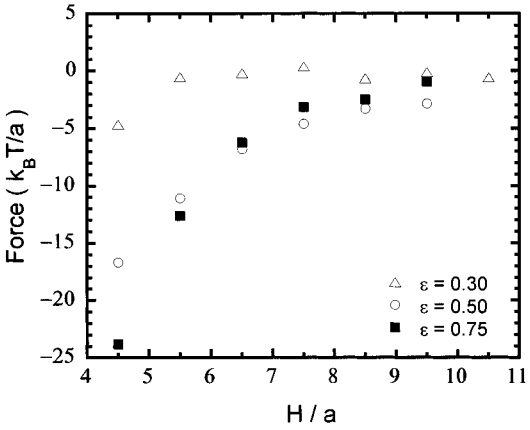

Figure 4. Force, f, as a function of the separation between surfaces, H/a, for different values of the adsorption energy.

is the probability that a bridge with s segments is stretched by a factor of approximately $H/as^{3/5}$ times its natural length. It is evident, from eq 1, that for $\epsilon = 1.0\ k_BT$ most of the bridges are stretched beyond their natural length, whereas for $\epsilon = 0.5\ k_BT$ there is a considerable amount (~20%) of large, loosely stretched bridges.

The tension in each strongly stretched bridge can be described by a law proposed by Pincus,[28] which in our context is[40]

$$f \sim \frac{H^{3/2}}{R_F^{5/2}}, \quad H > R_F \tag{6}$$

The restoring force of those bridges that are not strongly stretched is described by the springlike linear relation between force and separation:[41]

$$f \sim \frac{H}{R_F^{2}}, \quad H < R_F \tag{7}$$

The strong- and weak-stretching regimes described by eqs 6 and 7 have been observed in lattice Monte Carlo simulations on single chains stretched by a constant force applied at both ends.[15] These relations assume that the chain can take any conformation which ends exactly H layers from its starting point and hence do not account for the presence of the walls. It appears that eq 7 will not be entirely valid as a description of weakly

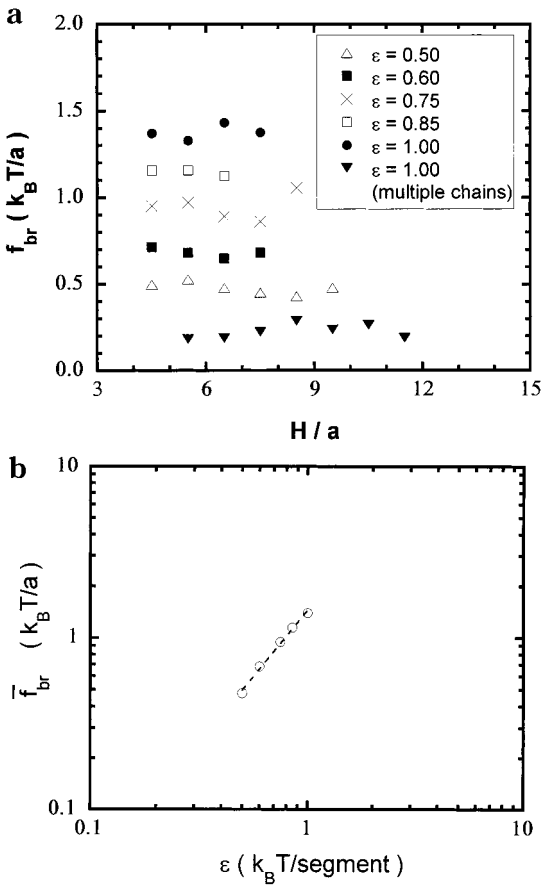

Figure 5. (a) Force per bridge, f_{br}, vs H/a for a range of adsorption energy. The lowest set of data correspond to a multiple chain system as described in section 3.4 and Figure 9. (b) Force per bridge vs adsorption energy, ϵ. The solid line corresponds to $f_{br} = 1.42\epsilon^{1.48}$.

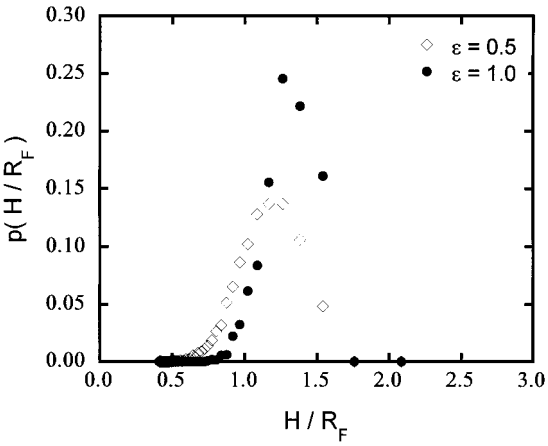

Figure 6. Probability, $p(x)$, that a bridge is stretched by a factor x, where $x = H/R \approx H/s^{3/5}$, and s is the number of segments in a bridge (see text). Separation is at $H/a = 5$. For $\epsilon = 0.5\ k_BT$, 80% of the bridges are strongly stretched ($H/R_F > 1$). For $\epsilon = 1.0\ k_BT$, 96% of the bridges are strongly stretched.

stretched bridges since, for this particular case, there would be a significant number of disallowed, wall-penetrating conformations.

The force profiles corresponding to the simulations in Figure 6 are shown in Figures 7 and 8. The dashed lines represent a theoretical comparison based on the distribution of bridges found in the simulation. If the polymer chain has $n(s)$ bridges with s segments each,

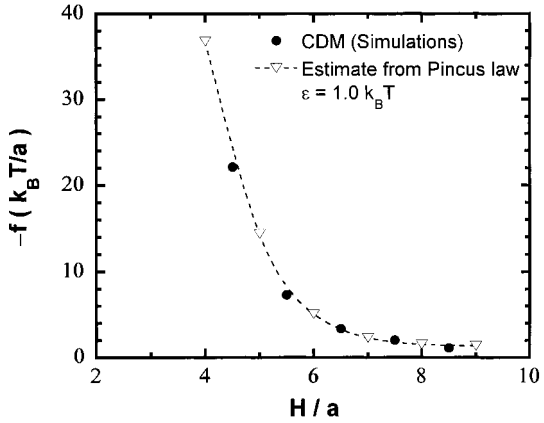

Figure 7. Attractive force between walls, $-f$, vs separation for $\epsilon = 1.0\ k_BT$.

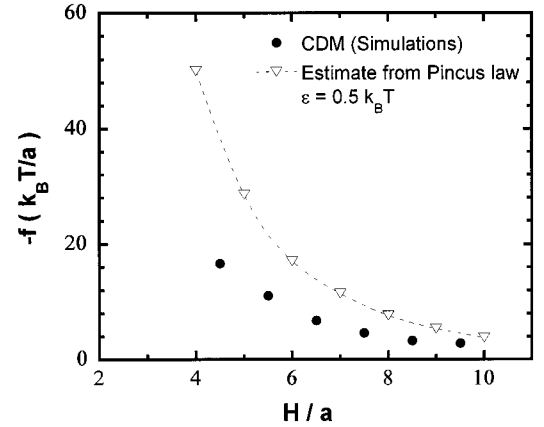

Figure 8. Attractive force between walls, $-f$, vs separation for $\epsilon = 0.5\ k_BT$.

the total force can be estimated as

$$f = \sum n(s)\, f_{br}(s) \tag{8}$$

where the force due to each bridge is calculated using either eq 6 or eq 7.

As is evident from Figure 8, the assumption that a system is governed completely by the elasticity of its bridges does not hold in cases where there is a significant number of weakly stretched bridges. In such cases, other effects such as steric forces (bridge−bridge interactions and interaction of bridges with the rest of the chain) and exclusion of conformations that penetrate the walls diminish the attraction. In multichain systems the presence of steric forces can go as far as to create an overall repulsion between the surfaces. The images shown in Figure 2 demonstrate the steric effects that exist in the cases of weak and strong adsorption. The prediction of force per bridge that scales with adsorption energy as shown in eq 1 is probably limited to conditions where the adsorption strength is high enough that almost every bridge is strongly stretched.

3.4. Scaling Relation for Pulling a Chain Off of a Surface. Testing eq 1 using standard experiments is difficult because of the difficulty of isolating the contributions from strongly stretched bridges from the overall measurement. Therefore, it is useful to conceive of methods to test eq 1 more directly. Pulling a chain off of a surface using an atomic force microscope may provide the type of information necessary to examine eq 1.

A theoretical analysis of an adsorbed (Gaussian) chain subjected to an external force has shown that the competition between stretching and adsorption leads to a rich behavior with first- and second-order transitions.[42] A simple scaling analysis for this problem was suggested recently for a weakly adsorbing, *ideal* chain.[43] In what follows we adapt this approach to obtain a scaling relation between the force and the adsorption energy for the case of strong stretching in a good solvent. First one determines the spatial extension ("thickness") D of an adsorbed chain following the arguments presented by de Gennes[41] by assuming the following free energy functional:

$$F = k_BT\,\frac{N}{(D/a)^{5/3}} - \epsilon N\frac{a}{D} = Nk_BT\left(\tilde{D}^{-5/3} - \frac{\theta}{\tilde{D}}\right) \tag{9}$$

where $\tilde{D} = D/a$ and $\theta = \epsilon/k_BT$. The first term describes the free energy of confinement for an adsorbed layer of N segments and is based on the argument that the chain is a sequence of blobs of extension, D, each with an energy k_BT. The second term is an estimate of energy due to the surface contacts assuming the chain segments are evenly distributed in the thickness D. One can now minimize the free energy with respect to $\tilde{D}$ to find the equilibrium layer thickness (see ref 41, Chapter 1):

$$\tilde{D}^* \simeq \theta^{-3/2} \tag{10}$$

For a chain being pulled by one of its segments, we modify the free energy functional in eq 9 as follows when there is a bridge with p segments:

$$\frac{F(p)}{k_BT} \sim -\theta^{5/2}(N - p) + \left(\frac{\tilde{H}}{p^{3/5}}\right)^{5/2} \tag{11}$$

where $\tilde{H} = H/a$. Equation 11 is arrived at by substituting $N - p$ for N and $\tilde{D}^*$ for D in eq 9 and by adding the second term on the right-hand side to describe the bridge between the surface and the AFM tip by the elastic free energy expression which corresponds to eq 6. The minus sign on the first term in eq 11 is necessary in order that the free energy of the adsorbed part of the chain decreases, rather than increases, with increasing chain length, temperature, and adsorption strength. The minimization of eq 11 with respect to the number of segments in the "tether" yields the equilibrium size of the tether:

$$p^* \sim \frac{\tilde{H}}{\theta} \tag{12}$$

The Helmholtz free energy $F(p)$ at $p = p^*$ is then used to find the equilibrium force:

$$\frac{f}{k_BT} \sim -\frac{\theta^{3/2}}{a} \tag{13}$$

It is not surprising that, as in the case of bridging between walls, the force is independent of separation and depends on adsorption energy through an exponent of 1.5 since the same type of balance between bridging and adsorbing segments exists. In addition to establishing a link between similar problems, this correspondence confirms that the physical content of the two scaling approaches (namely, the one presented here and the one by Ji et al.[5]) is the same, even though the

approach by Ji et al.[5] is based on an extension of mean-field calculations.

This scaling analysis suggests that an experiment may be designed to obtain direct information on the adsorption energies of surfaces from the measured bridging forces. Therefore, it is useful to consider how a direct comparison of the simulation results may be made with such experimental data. The correspondence between real chains and universal polymer models used in simulations depends mainly on the relative stiffness of the type of polymer being considered. For instance, for PEO in water (a good solvent) the lattice scale corresponds approximately to 0.6 nm, with each segment in the lattice containing about 1.6 ethylene oxide monomers. Then, our data for the force and adsorption strength of $(f, \epsilon) = (1.4\ k_BT/a, 1.0\ k_BT)$ would correspond to $(f, \epsilon) =$ (9 pN, 0.4 kcal/mol). It should be borne in mind that this estimate can be only as good as the accuracy of the correspondence between coarse-grained models and real chains. Therefore, the above comparison should be viewed mainly as an instructive example of the possibility for exploring surface/polymer characteristics.

We should caution, however, that eq 13 was developed under the assumption that the system remains at equilibrium, and hence the length of the tether between the surface and the AFM tip is allowed to adjust itself at each separation. In contrast, this is not usually the case in the experiments reported in the literature. That is, if the velocity of retraction of the AFM tip is large compared to the relaxation time of the adsorbed chain, the measured force would be determined by the appropriate force−length relationship (which follows the Pincus law for moderate forces and becomes model-dependent for large stretching), and eq 13 would not be valid anymore.

4. Concluding Remarks

4.1. Toward Multiple Chains. It is useful at this stage to comment on the case of multiple chains and contrast it with single chains. A detailed examination of multichain systems will be presented in the future; here we present preliminary results to highlight some similarities and differences the multichain problem has with the present study. Results are presented for the forces observed between two partially coated surfaces in a multichain system. The system consists of 200-segment chains in an athermal solvent between two adsorbing walls each with $\epsilon = 1.0\ k_BT$. A total of 12 chains are considered in a $40 \times 40 \times H$ lattice, corresponding to three monomers for every four surface sites. Since the equivalent adsorbed layer in equilibrium with a dilute solution has roughly one monomer for every surface site, this simulation corresponds to a starved surface. The results obtained for a range of separation distances are shown in Figure 9. Also shown in the figure is the theoretical curve from eq 8 based on summing the Pincus law prediction for single bridges of a given size by the number of bridges of that size. First, it can be seen that the net force observed from the simulations is attractive. However, the force observed falls well below the prediction based on eq 8, indicating that steric effects play a significant role in multichain systems. This is especially clear from a comparison with Figure 7, which shows that the Pincus law works well for an identical, but single-chain, system. Dividing the total force by the number of bridges yields,

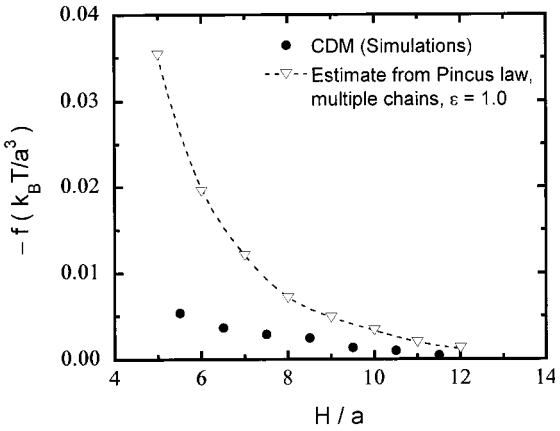

Figure 9. Attractive force between walls per unit area, $-f/A$, vs separation for $\epsilon = 1.0\ k_BT$ in a *multiple chain* system of 12 200-segment chains corresponding to a slightly undersaturated layer.

as in the single-chain cases, a roughly constant force (Figure 5a, bottom curve). The constancy implies that the behavior of bridging does not change significantly except for the addition of steric repulsion. Figure 5a for multiple chains explains the constant force per bridge observed experimentally by Swenson et al.[19,20] However, it should be borne in mind that the observed force per bridge cannot be related unequivocally to the adsorption energy of the surfaces, nor is it an indication that one has a collection of noninteracting bridges. The fact that the data for multiple chains at $\epsilon = 1.0\ k_BT$ are well below the corresponding single-chain case demonstrates the importance of steric interactions such as bridge−bridge interactions, bridge−loop interactions, etc.[44]

4.2. Summary. We have reported the results of lattice Monte Carlo simulations of a single chain in an athermal solvent confined between adsorbing surfaces. Our results are in good agreement with the picture suggested by the recent experiments of Swenson et al.[19,20] where a constant force per bridge was observed in an aqueous/clay/PEO system under equilibrium conditions. They are also in excellent agreement with the more directly related scaling analysis by Ji et al.[5] In particular, we observe the force per bridge, $f_{br} \sim (\epsilon/a)^m$, with the exponent, m, roughly equal to 1.5. The details of bridging interactions are accessible in greater detail when the actual distribution of bridges is examined, as illustrated in the paper. The results presented in the paper provide stronger guidelines for distinguishing between the strong- and weak-stretching regimes. For the latter, there is as yet no sufficient theoretical model available. Finally, we note that the force of strongly stretched bridges is very similar to the force of (quasi-static) retraction of a chain off of a surface with the tip of an atomic force microscope. The adsorption energy of real surfaces is historically a difficult quantity to measure. Perhaps it can now be inferred from the retraction force.

Acknowledgment. The authors acknowledge partial financial support from the National Science Foundation through the Engineering Research Center for Particle Science and Technology at the University of Florida (Grant NSF EEC-9402989).

References and Notes

(1) de Joannis, J.; Jimenez, J.; Rajagopalan, R.; Bitsanis, I. *Europhys. Lett.* **2000**, *51*, 41.

(2) de Gennes, P.-G. *Macromolecules* **1982**, *15*, 492.
(3) Klein, J.; Pincus, P. *Macromolecules* **1982**, *15*, 1129. Ingersent, K.; Klein, J.; Pincus, P. *Macromolecules* **1986**, *19*, 1374; **1990**, *23*, 548.
(4) Rossi, G.; Pincus, P. *Macromolecules* **1989**, *22*, 276.
(5) Ji, H.; Hone, D.; Pincus, P.; Rossi, G. *Macromolecules* **1990**, *23*, 698.
(6) Brooks, J. T.; Cates, M. E. *Macromolecules* **1992**, *25*, 391.
(7) Bonet-Avalos, J.; Johner, A.; Joanny, J.-F. *J. Chem. Phys.* **1994**, *101*, 9181.
(8) Semenov, A. N.; Joanny, J.-F.; Johner, A.; Bonet-Avalos, J. *Macromolecules* **1997**, *30*, 1479.
(9) Mendez-Alcaraz, J. M.; Johner, A.; Joanny, J.-F. *Macromolecules* **1998**, *31*, 8297.
(10) Scheutjens, J. M. H. M.; Fleer, G. J. *Macromolecules* **1985**, *18*, 1882.
(11) de Gennes, P.-G. In *Physical Basis of Cell−Cell Adhesion*; Bongard, P., Ed.; CRC Press Inc.: Boca Raton, FL, 1988.
(12) Klein, J.; Rossi, G. *Macromolecules* **1998**, *31*, 1979.
(13) Misra, S.; Mattice, W. L. *Macromolecules* **1994**, *27*, 2058.
(14) van Giessen, S.; Szleifer, I. *J. Chem. Phys.* **1995**, *102*, 9069.
(15) Hölzl, T.; Wittkop, M.; Kreitmeier, S.; Göritz, D. *J. Chem. Phys.* **1997**, *106*, 7792.
(16) Luckham, P. F.; Klein, J. *J. Chem. Soc., Faraday Trans.* **1990**, *86*, 1363.
(17) Luckham, P. F. *Adv. Colloid Interface Sci.* **1991**, *34*, 191.
(18) Braithwaite, G. J. C.; Howe, A.; Luckham, F. *Langmuir* **1996**, *12*, 4224.
(19) Swenson, J.; Smalley, M. V.; Hatharasinghe, H. L. M. *Phys. Rev. Lett.* **1998**, *26*, 5840.
(20) Swenson, J.; Smalley, M. V.; Hatharasinghe, H. L. M. *J. Chem. Phys.* **1999**, *110*, 9750.
(21) DiMarzio, E. A.; Rubin, R. J. *J. Chem. Phys.* **1971**, *55*, 4318.
(22) Gaylord, R. J.; Lohse, D. J. *J. Chem. Phys.* **1976**, *65*, 2779.
(23) Pfau, A.; Schrepp, W.; Horn, D. *Langmuir* **1999**, *15*, 3219.
(24) Li, H.; Liu, B.; Zhang, X.; Gao, C.; Shen, J.; Zou, G. *Langmuir* **1999**, *15*, 2120.
(25) Ortiz, C.; Hadziioannou, G. *Macromolecules* **1999**, *32*, 780.
(26) Fleer, G.; Cohen Stuart, M.; Scheutjens, J.; Cosgrove, T.; Vincent, B. *Polymers at Interfaces*; Chapman and Hall: London, 1993.
(27) It is believed that polymer physisorption is characterized by extremely long adsorption times (of the order of hours or days) as shown, for example, in the experiments of Luckham and Klein on PEO.[16] A few hours after adding polymer to a good solvent, an overall attractive interaction between surfaces is observed. A steady state is found many hours later, in which an overall repulsion is consistently observed. There is little knowledge beyond this of the kinetics of physisorption, especially on the amount and structure of polymer chains at the surface during the incubation phase.
(28) Pincus, P. *Macromolecules* **1976**, *9*, 386.
(29) The importance of tails diminishes as the chain length becomes large since the numbers of bridges and loops increase while the number of tails is always two. The tail size cannot grow indefinitely since tails will form bridges once their size is comparable to the gap width.
(30) Siepmann, J. I.; Frenkel, D. *Mol. Phys.* **1992**, *75*, 59.
(31) Rosenbluth, M. N.; Rosenbluth, A. W. *J. Chem. Phys.* **1955**, *23*, 356.
(32) Jimenez, J.; Rajagopalan, R. *Eur. Phys. J. B* **1998**, *5*, 237.
(33) Bennet, C. *J. Comput. Phys.* **1976**, *22*, 245.
(34) The idea of using repulsive walls was first introduced by Dickman and co-workers,[35] who used a thermodynamic integration method to estimate the change in free energy when moving the wall from $z = H$ to $z = H - 1$. Dickman's method uses only the *average* number of contacts, consequently requiring more simulations than the CDM, in which the entire distribution of contacts is used.
(35) Dickman, R.; Hong, D. *J. Chem. Phys.* **1991**, *95*, 4650. Dickman, R.; Anderson, P. E. *J. Chem. Phys.* **1993**, *99*, 3112.
(36) We actually proceed in the reverse order from step iii to step i since in that case one can use the final configuration from step iii as the initial configuration for step i, thus reducing the time required to generate a new system.
(37) The concentration profile will be certainly affected, but properties such as the lateral component of the radius of gyration would not.
(38) This observation is actually confirmed by the analysis of the segment−concentration profile between the walls.
(39) The exact relation we use for the Flory radius is $R_F/a = 0.99N^{0.593}$, which is suitable for chain lengths above 20 on a simple cubic lattice.
(40) The upper limit for the validity of this equation has been established through simulations (e.g., Hölzl et al.)[15] to be approximately $2R_F$. When the chain is stretched to twice its natural size, the force becomes model-dependent.
(41) de Gennes, P.-G. *Scaling Concepts in Polymer Physics*; Cornell University Press: Ithaca, NY, 1979.
(42) Skvortsov, A. M.; Gorbunov, A. A.; Klushin, L. I. *J. Chem. Phys.* **1994**, *100*, 2325. Di Marzio, E. A.; Guttman, C. M. *J. Chem. Phys.* **1991**, *95*, 1189. Klushin, L. I.; Skvortsov, A. M.; Gorbunov, A. A. *Phys. Rev. E* **1997**, *56*, 1511.
(43) Haupt, B. J.; Ennis, J.; Sevick, E. M. *Langmuir* **1999**, *15*, 3886.
(44) The simulations also show that the average number and size of the bridges (per unit area) have the same exponential decay and linear increase (respectively) with separation as in the single-chain case. This is in agreement with the scaling results of Ji et al.[5] for bridging in a semidilute polymer solution. More details will be presented in a later publication.

MA000564N